Supplementary information

Supplementary files:
- Figure S1: Pedigree of the family with five affected individuals carrying p.(Arg2579His)
- Figure S2: Variant p.(Glu2522Lys) in individuals 13 and 14 is equivalent to Yoda variant p.(Glu2502Lys)
- Figure S3: Four variants are located at 3 residues in predicted destruction motifs
- Figure S4: *ANKRD11* missense variants affecting arginine residues in RD2 are overrepresented in the cohort
- Figure S5: Quantification of ANKRD11 nuclear speckles.
- Figure S6: EGFP-ANKRD11 protein expression in transiently transfected HEK293T/17 cells.
- Figure S7: Relative expression ANKRD11 variants as EGFP-fusion protein in HEK293T/17 cells treated with (A) 50µg/ml cycloheximide (CHX) or (B) 5µg/ml proteasome inhibitor MG132.
- Figure S8: Potential effects on cryptic splice sites
- Table S1: ANKRD11 missense variants reported in literature (provided separately)
- Table S2: Clinical information per individual (provided separately)
- Table S3: Simplified clinical features based on HPO-data using the Wang algorithm and clustering of individuals (provided separately)
- Table S4: List of primers & antibodies (provided separately)
- Table S5: List of variants, including annotations and classification based on ACMG/AMP (provided separately)
- Table S6: Destruction motifs (provided separately)
- Supplementary_HPO-data_in_JSON (provided separately)

SUPPLEMENTARY INFORMATION RELATED TO INTRODUCTION

ANKRD11 missense variants reported in literature

Individuals with *ANKRD11* missense variants reported in literature are listed in Table S1 [1-20].

SUPPLEMENTARY METHODS

Identification of *ANKRD11* variants, clinical characterization and *in silico* predictions

Individuals with (likely) pathogenic *ANKRD11* missense variants were identified through international collaborations facilitated by MatchMaker Exchange [21], the Decipher Database [22], the Solve-RD consortium and RD-connect [23]. Variants were identified by WES or Sanger sequencing as previously described [24, 25]. We annotated variants in the context of genome build GRCh37/Hg19, using transcript reference sequence NM_013275.6 and protein reference sequence NP_037407.4. Pathogenicity of variants was assessed by the following *in silico* tools: CADD-PHRED V1.6 [26], PhyloP 2015 [27], GERP 2013 [28], Align GVGD v2007 [29], SIFT v6.2.0 [30], MutationTaster v2013 [31], Grantham [32], Metadome [33] and SpliceAI [34]. ANKRD11 domain information is provided in Table S5B [13, 35-39]. The presence of degron motifs was analysed with ProViz and presented in Table S6 [40]. Variants were classified according to ACMG/AMP guidelines [41]. Individuals were clinically characterized by reviewing medical files, and/or revising the phenotypes in outpatient clinics. Phenotypic fit to the KBG-associated clinical spectrum was assessed by two medical geneticists with expertise in KBG syndrome, based on diagnostic criteria [42] and frequently described features in four large cohorts [42-45]. We obtained informed consent to publish unidentifiable data for all individuals reported in this study. Specific consent was obtained for publication of clinical photographs. Consent procedures were in accordance with the Declaration of Helsinki and local ethical guidelines of participating centres.

Human Phenotype Ontology (HPO)-based phenotype clustering analysis

To quantify potential differences between phenotypic features of individuals with ANKRD11 missense variants and individuals with ANKRD11 PTVs or microdeletions, HPO-based clustering analysis was performed as previously described [46]. Clinical data of 29 individuals carrying ANKRD11 missense variants, and of 35 individuals with KBG syndrome caused by *ANKRD11* PTVs or 16q24 microdeletions affecting *ANKRD11* only (Table S2 [1, 12, 42, 43], Supplementary JSON) obtained from the Radboudumc expert centre for rare neurodevelopmental disorders via Biobank Genetics and Rare Disease were standardized using HPO terminology (release 2018-12-21) [47] in PhenoTips (https://github.com/phenotips/phenotips, version 1.4.1) [48]. To avoid interobserver bias, all standardization of clinical data to HPO terminology was performed by the same clinician. In brief, semantic similarity between all HPO terms was calculated with the Wang algorithm in the HPOSim R-package [49, 50]. Terms were grouped and replaced by an overarching new feature when having a similarity score ≥0.5 (Table S3). To quantify a potential difference between cases with missense variants and cases with PTVs/microdeletions, we used Partitioning Around Medoids (PAM) clustering [51]. This analysis defines two clusters in the total available HPO-data. The algorithm is agnostic both to the size of the clusters as well as to the observed variant type of the individuals (correct labels), as the size of the clusters is not defined upfront, and the algorithm is not provided with the correct labels (PTV or missense). After the cluster analysis, the correct labels are used to establish for how many individuals the predicted cluster corresponds with the observed variant, generating a score. To determine the statistical significance of the score of the cluster analysis, a permutation test (100,000x) is performed, that randomly shuffles the correct labels and repeats the analysis. The score of the cluster analysis on the true cohort is then compared to the scores generated by the permutation test – enabling the calculation of a p-value.

All code is available online at https://github.com/ldingemans/HPO_clustering_Wang. Furthermore, the results of this clustering analysis, the permutation test and the calculation of the corresponding p-value are available in Table S3A-C.

Data of individuals obtained from the Radboudumc Biobank and Radboudumc KBG national referral centre

To compare the individuals with ANRKD11 missense variants observed in the cohort to KBG syndrome resulting from PTVs and 16q24.3 microdeletions, we used information on genotype and phenotype of 35 individuals diagnosed with KBG syndrome obtained from the Radboudumc Biobank Genetics and Rare Disease (https://www.radboudumc.nl/en/research/radboud-technology-centers/radboud-biobank) and the Radboudumc KBG national referral centre.

The 35 individuals obtained from the Radboudumc Biobank are a representative subset of all individuals with KBG syndrome that are in clinical care of the Radboudumc KBG national referral centre (https://www.radboudumc.nl/en/centers-of-clinical-expertise/centers-of-clinical-expertise-for-rare-diseases/rare-congenital-developmental-disorders), capturing the full phenotypic spectrum of KBG syndrome, including mild and subclinical presentations. This group of 35 individuals comprises all individuals with KBG syndrome caused by PTVs or 16q24.3 microdeletions that consented for further research studies using clinical and genetic data. Of the 35 individuals, 18 were male and 17 female, with an age range of 3 to 73 years. Genotypically, three individuals had a 16q24.3 microdeletion that only comprised (part of) *ANKRD11*, 24 individuals carried frameshift variants, and eight individuals had a nonsense variant. Of the 32 single nucleotide variants and indels, 31 located to the long exon 9, introducing a premature stop codon that is predicted to result in escape from the nonsense-mediated decay (NMD) pathway, whereas only one variant is predicted to trigger NMD [52,

53]. Variants were shown to be *de novo* in 23 individuals. For four individuals, the variant occurred in a familial context, and for the final eight, inheritance could not be established.

Spatial clustering analysis of missense variants

25 of the 29 observed missense variants were included in spatial clustering analysis, after removal of four variants because of familial occurrence. The geometric mean was computed over the locations of observed missense variants in the cDNA of *ANKRD11* (7,992 bp) and subsequently compared to each of the geometric means of 1,000,000 permutations of randomly redistributing the variant locations over the total coding sequence of *ANKRD11*. A *p*-value was obtained by calculating how often the observed geometric distance was smaller than the permutated geometric mean distance [54, 55] and considered significant if <0.05.

Immunoblotting

Whole-cell lysates were prepared as described previously [56]. Total protein was quantified using the Pierce BCA protein assay kit (Thermo Fisher). Proteins were resolved on 4–15% Tris-Glycine gels and transferred to PDVF membranes (Bio-Rad). After blotting, membranes were incubated overnight at 4˚C with the appropriate primary antibodies. Membrane were then incubated with HRP-conjugated secondary antibodies. Proteins were visualized using the Novex ECL Chemiluminescent Substrate Reagent kit (Invitrogen) or SuperSignal West Femto Maximum Sensitivity Substrate (Thermo Fisher) and the ChemiDoc XRS+ System (Bio-Rad). A list of antibodies used can be found in Table S4.

SUPPLEMENTARY RESULTS

ANKRD11 missense variants cause syndromic neurodevelopmental phenotypes

In addition to the most frequently observed phenotypic features described in the manuscript, individuals presented with a variety of additional features (summarized in Table 1 with details provided in Table S2). We observed seizures in six cases (6/27, 22.2%), ranging in severity from absence seizures to refractory complex focal seizures. Additional neurological features were predominantly mild, with sleep disturbances (8/26, 30.8%) and hypotonia (10/24, 41.7%) most frequently reported. Commonly observed behavioral problems included ADHD or hyperactivity (18/26, 69.2%), ASD (9/25, 36%) and anxiety (9/24, 37.5%), together with a spectrum of additional behavioral symptoms. Although most individuals were born at term (23/24, 95.8%), both pre- and perinatal complications were prevalent (11/24, 45.8% and 15/26, 57.7% respectively), including maternal pregnancy-related illness, a variety of ultrasound abnormalities, complicated delivery and asphyxia. Short stature was seen in over half of the cohort (15/28, 53.6%), explained by growth hormone deficiency in only two individuals, and seven cases presented with abnormal head circumference (macrocephaly 1/27, 3.7%; microcephaly 6/27, 22.2%). Congenital heart defects occurred in 32% of individuals (8/25), mostly consisting of atrial and/or ventricular septal defects and cardiac valve abnormalities. Cryptorchidism was observed in 20% of male individuals (3/15), and other urogenital abnormalities included duplication of the kidney or renal collecting system and hypospadias. The most prominent problems of the gastrointestinal tract were feeding difficulties (9/27, 33.3%), constipation (6/27, 22.2%) and gastroesophageal reflux disease (3/27, 11.1%). Over half of all individuals showed delayed bone maturation (8/14, 57.1%), but other abnormalities of the skeletal system were not frequently reported. Abnormalities of vision occurred in 50% (13/26) of individuals, comprising hypermetropia, myopia, astigmatism and strabismus. Hearing loss, resulting from recurrent or chronic otitis media, stapes ankylosis or ear atelectasis, was also prevalent (11/28, 39.3%). Only two individuals had a cleft palate, and two individuals were affected by velopharyngeal insufficiency.

Additionally, a wide range of other abnormalities was observed at low frequencies (Table S2), most remarkably choanal atresia (individual 4) and ileal atresia (individual 19).

SUPPLEMENTARY REFERENCES

1. Kaplanis, J., et al., *Evidence for 28 genetic disorders discovered by combining healthcare and research data.* Nature, 2020. **586**(7831): p. 757-762.
2. Alfieri, P., et al., *Cognitive and Adaptive Characterization of Children and Adolescents with KBG Syndrome: An Explorative Study.* J Clin Med, 2021. **10**(7).
3. Butler, M.G., et al., *Whole exome sequencing in females with autism implicates novel and candidate genes.* Int J Mol Sci, 2015. **16**(1): p. 1312-35.
4. Guevara-Aguirre, J., et al., *Branding of subjects affected with genetic syndromes of severe short stature in developing countries.* BMJ Case Rep, 2020. **13**(2).
5. Kang, Y., et al., *A heterozygous point mutation of the ANKRD11 (c.2579C>T) in a Chinese patient with idiopathic short stature.* Mol Genet Genomic Med, 2019. **7**(12): p. e988.
6. Kutkowska-Kaźmierczak, A., et al., *Wide Fontanels, Delayed Speech Development and Hoarse Voice as Useful Signs in the Diagnosis of KBG Syndrome: A Clinical Description of 23 Cases with Pathogenic Variants Involving the ANKRD11 Gene or Submicroscopic Chromosomal Rearrangements of 16q24.3.* Genes (Basel), 2021. **12**(8).
7. Li, Q., et al., *Comprehensive analysis of clinical spectrum and genotype associations in Chinese and literature reported KBG syndrome.* Transl Pediatr, 2021. **10**(4): p. 834-842.
8. Meyer, R., et al., *Targeted Next Generation Sequencing Approach in Patients Referred for Silver-Russell Syndrome Testing Increases the Mutation Detection Rate and Provides Decisive Information for Clinical Management.* J Pediatr, 2017. **187**: p. 206-212.e1.

9. Miyatake, S., et al., *ANKRD11 variants cause variable clinical features associated with KBG syndrome and Coffin-Siris-like syndrome.* J Hum Genet, 2017. **62**(8): p. 741-746.
10. Murray, N., et al., *KBG syndrome: An Australian experience.* Am J Med Genet A, 2017.
11. Scarano, E., et al., *Novel Mutations and Unreported Clinical Features in KBG Syndrome.* Mol Syndromol, 2019. **10**(3): p. 130-138.
12. van Dongen, L.C.M., et al., *Exploring the behavioral and cognitive phenotype of KBG syndrome.* Genes Brain Behav, 2019: p. e12553.
13. Walz, K., et al., *Characterization of ANKRD11 mutations in humans and mice related to KBG syndrome.* Hum Genet, 2015. **134**(2): p. 181-90.
14. Xia, F., et al., *De novo truncating mutations in AHDC1 in individuals with syndromic expressive language delay, hypotonia, and sleep apnea.* Am J Hum Genet, 2014. **94**(5): p. 784-9.
15. Xu, M., et al., *A Chinese patient with KBG syndrome and a 9q31.2-33.1 microdeletion.* Eur J Med Genet, 2013. **56**(5): p. 245-50.
16. Yan, H., et al., *Targeted next generation sequencing in 112 Chinese patients with intellectual disability/developmental delay: novel mutations and candidate gene.* BMC Med Genet, 2019. **20**(1): p. 80.
17. Zhang, T., et al., *Two loss-of-function ANKRD11 variants in Chinese patients with short stature and a possible molecular pathway.* Am J Med Genet A, 2021. **185**(3): p. 710-718.
18. Quaio, C., et al., *Diagnostic power and clinical impact of exome sequencing in a cohort of 500 patients with rare diseases.* Am J Med Genet C Semin Med Genet, 2020. **184**(4): p. 955-964.
19. Benson, K.A., et al., *A comparison of genomic diagnostics in adults and children with epilepsy and comorbid intellectual disability.* Eur J Hum Genet, 2020. **28**(8): p. 1066-1077.

20. Guo, L., et al., *KBG Syndrome: Prospective Videoconferencing and Use of AI-driven Facial Phenotyping in 25 New Patients.* medRxiv, 2021: p. 2021.11.18.21266480.
21. Sobreira, N., et al., *GeneMatcher: a matching tool for connecting investigators with an interest in the same gene.* Hum Mutat, 2015. **36**(10): p. 928-30.
22. Firth, H.V., et al., *DECIPHER: Database of Chromosomal Imbalance and Phenotype in Humans Using Ensembl Resources.* Am J Hum Genet, 2009. **84**(4): p. 524-33.
23. Thompson, R., et al., *RD-Connect: an integrated platform connecting databases, registries, biobanks and clinical bioinformatics for rare disease research.* J Gen Intern Med, 2014. **29 Suppl 3**(Suppl 3): p. S780-7.
24. de Ligt, J., et al., *Diagnostic exome sequencing in persons with severe intellectual disability.* N Engl J Med, 2012. **367**(20): p. 1921-9.
25. Guillen Sacoto, M.J., et al., *De Novo Variants in the ATPase Module of MORC2 Cause a Neurodevelopmental Disorder with Growth Retardation and Variable Craniofacial Dysmorphism.* Am J Hum Genet, 2020. **107**(2): p. 352-363.
26. Rentzsch, P., et al., *CADD: predicting the deleteriousness of variants throughout the human genome.* Nucleic Acids Res, 2019. **47**(D1): p. D886-d894.
27. Siepel, A., et al., *Evolutionarily conserved elements in vertebrate, insect, worm, and yeast genomes.* Genome Res, 2005. **15**(8): p. 1034-50.
28. Davydov, E.V., et al., *Identifying a high fraction of the human genome to be under selective constraint using GERP++.* PLoS Comput Biol, 2010. **6**(12): p. e1001025.
29. Tavtigian, S.V., et al., *Comprehensive statistical study of 452 BRCA1 missense substitutions with classification of eight recurrent substitutions as neutral.* J Med Genet, 2006. **43**(4): p. 295-305.
30. Vaser, R., et al., *SIFT missense predictions for genomes.* Nat Protoc, 2016. **11**(1): p. 1-9.
31. Schwarz, J.M., et al., *MutationTaster2: mutation prediction for the deep-sequencing age.* Nat Methods, 2014. **11**(4): p. 361-2.

32. Grantham, R., *Amino acid difference formula to help explain protein evolution.* Science, 1974. **185**(4154): p. 862-4.

33. Wiel, L., et al., *MetaDome: Pathogenicity analysis of genetic variants through aggregation of homologous human protein domains.* Hum Mutat, 2019. **40**(8): p. 1030-1038.

34. Jaganathan, K., et al., *Predicting Splicing from Primary Sequence with Deep Learning.* Cell, 2019. **176**(3): p. 535-548.e24.

35. Neilsen, P.M., et al., *Identification of ANKRD11 as a p53 coactivator.* J Cell Sci, 2008. **121**(Pt 21): p. 3541-52.

36. Zhang, A., et al., *Identification of a novel family of ankyrin repeats containing cofactors for p160 nuclear receptor coactivators.* J Biol Chem, 2004. **279**(32): p. 33799-805.

37. Zhang, A., C.W. Li, and J.D. Chen, *Characterization of transcriptional regulatory domains of ankyrin repeat cofactor-1.* Biochem Biophys Res Commun, 2007. **358**(4): p. 1034-40.

38. Morel Swols, D., J. Foster, 2nd, and M. Tekin, *KBG syndrome.* Orphanet J Rare Dis, 2017. **12**(1): p. 183.

39. Neilsen, P.M. *Functional Analysis of ANKRD11 and FBXO31: Two Candidate Tumour Suppressor Genes from the 16q24.3 Breast Cancer Loss of Heterozygosity Region*. 2008; Available from: https://digital.library.adelaide.edu.au/dspace/bitstream/2440/59014/8/02whole.pdf.

40. Jehl, P., et al., *ProViz-a web-based visualization tool to investigate the functional and evolutionary features of protein sequences.* Nucleic Acids Res, 2016. **44**(W1): p. W11-5.

41. Richards, S., et al., *Standards and guidelines for the interpretation of sequence variants: a joint consensus recommendation of the American College of Medical Genetics and Genomics and the Association for Molecular Pathology.* Genet Med, 2015. **17**(5): p. 405-24.

42. Low, K., et al., *Clinical and genetic aspects of KBG syndrome.* Am J Med Genet A, 2016. **170**(11): p. 2835-2846.

43. Ockeloen, C.W., et al., *Further delineation of the KBG syndrome caused by ANKRD11 aberrations.* Eur J Hum Genet, 2015. **23**(9): p. 1270.

44. Goldenberg, A., et al., *Clinical and molecular findings in 39 patients with KBG syndrome caused by deletion or mutation of ANKRD11.* Am J Med Genet A, 2016. **170**(11): p. 2847-2859.

45. Gnazzo, M., et al., *KBG syndrome: Common and uncommon clinical features based on 31 new patients.* Am J Med Genet A, 2020. **182**(5): p. 1073-1083.

46. den Hoed, J., et al., *Mutation-specific pathophysiological mechanisms define different neurodevelopmental disorders associated with SATB1 dysfunction.* Am J Hum Genet, 2021. **108**(2): p. 346-356.

47. Köhler, S., et al., *Expansion of the Human Phenotype Ontology (HPO) knowledge base and resources.* Nucleic Acids Res, 2019. **47**(D1): p. D1018-d1027.

48. Girdea, M., et al., *PhenoTips: patient phenotyping software for clinical and research use.* Hum Mutat, 2013. **34**(8): p. 1057-65.

49. Deng, Y., et al., *HPOSim: an R package for phenotypic similarity measure and enrichment analysis based on the human phenotype ontology.* PLoS One, 2015. **10**(2): p. e0115692.

50. Wang, J.Z., et al., *A new method to measure the semantic similarity of GO terms.* Bioinformatics, 2007. **23**(10): p. 1274-81.

51. Kaufman, L. and P.J. Rousseeuw. *Clustering by means of medoids* *https://wis.kuleuven.be/stat/robust/papers/publications-1987/kaufmanrousseeuw-clusteringbymedoids-l1norm-1987.pdf*. 1987 [cited 2020].

52. Lindeboom, R.G., F. Supek, and B. Lehner, *The rules and impact of nonsense-mediated mRNA decay in human cancers.* Nat Genet, 2016. **48**(10): p. 1112-8.

53. Lindeboom, R.G.H., et al., *The impact of nonsense-mediated mRNA decay on genetic disease, gene editing and cancer immunotherapy.* Nat Genet, 2019. **51**(11): p. 1645-1651.

54. Lelieveld, S.H., et al., *Meta-analysis of 2,104 trios provides support for 10 new genes for intellectual disability.* Nat Neurosci, 2016. **19**(9): p. 1194-6.

55. Lelieveld, S.H., et al., *Spatial Clustering of de Novo Missense Mutations Identifies Candidate Neurodevelopmental Disorder-Associated Genes.* Am J Hum Genet, 2017. **101**(3): p. 478-484.

56. Wong, M.M.K., et al., *Neurodegeneration in SCA14 is associated with increased PKCγ kinase activity, mislocalization and aggregation.* Acta Neuropathol Commun, 2018. **6**(1): p. 99.

Figure S1: Pedigree of the family with five individuals carrying p.(Arg2579His)

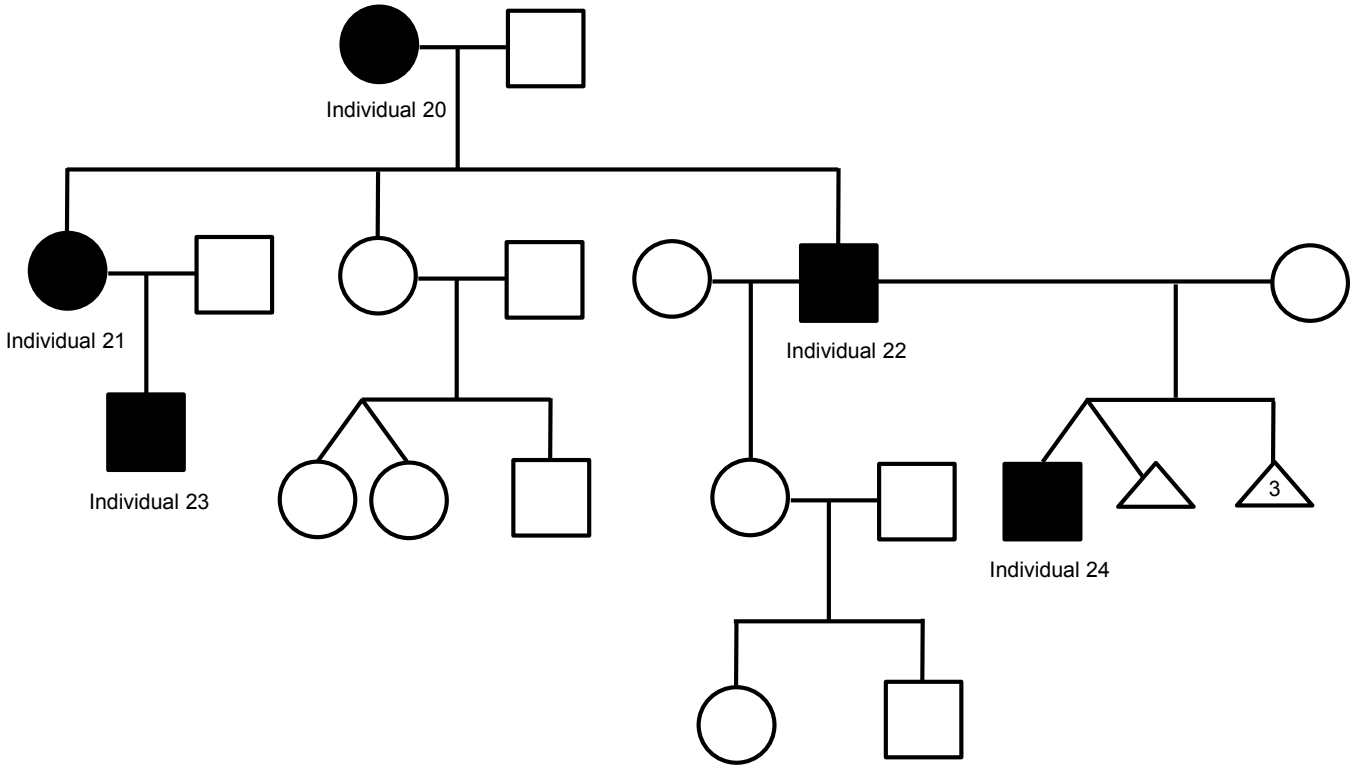

Figure S2: Variant p.(Glu2522Lys) in individuals 13 and 14 is equivalent to Yoda variant p.(Glu2502Lys)

Alignment of human ANKRD11 (Q6UB99) and mouse Ankrd11 (E9Q4F7) using CLUSTAL O(1.2.4) multiple sequence alignment. De human p.(Glu2522Lys) variant and Yoda mouse variant p.(Glu2502Lys) are marked.

```
SP|Q6UB99|ANR11_HUMAN MPKGGCPKAPQQEELPLSSDMVEKQTGKKDKDKVSLTKTPKLERGDGGKEVRERASKRKL 60
SP|E9Q4F7|ANR11_MOUSE MPKGGCSKTPQQEDFALSNDMVEKQTGKKDKDKVSLTKTPKLDRSDGGKEVRERATKRKL 60
                       ****** *:****:: **.**********************:*.**********:****

SP|Q6UB99|ANR11_HUMAN PFTAGANGEQKDSDTEKQGPERKRIKKEPVTRKAGLLFGMGLSGIRAGYPLSERQQVALL 120
SP|E9Q4F7|ANR11_MOUSE PFTVGANGEQKDSDTEKQGPERKRIKKEPVARKSGLLFGMGLSGIRAGYPLSERQQVALL 120
                       ***.**************************:**:************************

SP|Q6UB99|ANR11_HUMAN MQMTAEESANSPVDTTPKHPSQSTVCQKGTPNSASKTKDKVNKRNERGETRLHRAAIRGD 180
SP|E9Q4F7|ANR11_MOUSE MQMTAEESANSPVDTTPKHPSQSTVCQKGTPNSASKTKDKVNKRNERGETRLHRAAIRGD 180
                       ************************************************************

SP|Q6UB99|ANR11_HUMAN ARRIKELISEGADVNVKDFAGWTALHEACNRGYYDVAKQLLAAGAEVNTKGLDDDTPLHD 240
SP|E9Q4F7|ANR11_MOUSE ARRIKELISEGADVNVKDFAGWTALHEACNRGYYDIAKQLLAAGAEVNTKGLDDDTPLHD 240
                       ************************************:************************

SP|Q6UB99|ANR11_HUMAN AANNGHYKVVKLLLRYGGNPQQSNRKGETPLKVANSPTMVNLLLGKGTYTSSEESSTESS 300
SP|E9Q4F7|ANR11_MOUSE AANNGHYKVVKLLLRYGGNPQQSNRKGETPLKVANSPTMVNLLLGKGTYTSSEESSTESS 300
                       ************************************************************

SP|Q6UB99|ANR11_HUMAN EEEDAPSFAPSSSVDGNNTDSEFEKGLKHKAKNPEPQKATAPVKDEYEFDEDDEQDRVPP 360
SP|E9Q4F7|ANR11_MOUSE EEEDAPSFAPSSSVDGNNTDSEFEKGLKLKAKNPEPQKTVTPVKDEYEFDEDDEQDRVPP 360
                       *************************** *********:.:********************

SP|Q6UB99|ANR11_HUMAN VDDKHLLKKDYRKETKSNSFISIPKMEVKSYTKNNTIAPKKASHRILSDTSDEEDASVTV 420
SP|E9Q4F7|ANR11_MOUSE VDDKHLLKKDYRKEAKANSFISIPKMEVKSYSKNNTLAPKKAAHRILSDTSDEEDVSVSI 420
                       **************:*:**************:****:*****:************.**::

SP|Q6UB99|ANR11_HUMAN GTGEKLRLSAHTILPGSKTREPSNAKQQKEKNKVKKKRKKETKGREVRFGKRSDKFCSSE 480
SP|E9Q4F7|ANR11_MOUSE GAGEKLRLSAHTMLPGSKARESSSSRQQKEKNKLKKKRKKETKGKEVRFGKRSDKFCSSG 480
                       *:**********:*****:** *.::*******:**********:**************

SP|Q6UB99|ANR11_HUMAN SESESSESGEDDRDSLGSSGCLKGSPLVLKDPSLFSSLSASSTSSHGSSAAQKQNPSHTD 540
SP|E9Q4F7|ANR11_MOUSE SESESSESEEDDGDSVGSSGCLKGSPLVLKDPSLFSSLSASSTSSHGSAVAQKHGSGHTD 540
                       ******** *** **:**********************************:.***:. .***

SP|Q6UB99|ANR11_HUMAN QHTKHWRTDNWKTISSPAWSEVSSLSDSTRTRLTSESDYSSEGSSVESLKPVRKRQEHRK 600
SP|E9Q4F7|ANR11_MOUSE QHTKHWRTDNWKAISSPAWSEVSSLSDSSRTGLTSESDCSSEGSSVESLKPTRRKQEHRK 600
                       ************:***************:** ****** ************.*::*****

SP|Q6UB99|ANR11_HUMAN RASL----SEKKSPFLSSAEGAVPKLDKEGKVVKKHKTKHKHKNKEKGQCSISQELKLKS 656
SP|E9Q4F7|ANR11_MOUSE RGVLQSAPSEKRSSFHPCTDGAVPKLDKEGKVVKKHKTKHKHKHKEKGQCSVSQELKLKS 660
                       *. *    ***:* *  .::**********************:*******:********

SP|Q6UB99|ANR11_HUMAN FTYEYEDSKQKSDKAILLENDLSTENKLKVLKHDRDHFKKEEKLSKMKLEEKEWLFKDEK 716
SP|E9Q4F7|ANR11_MOUSE FTYEYEDSKQKSDKAILLESDLSTENKLKVLKHDREHLKKEDKLGRMKPEDKDWLFKDEK 720
                       *******************.***************:*:***:**.:** *:*:*******

SP|Q6UB99|ANR11_HUMAN SLKRIKDTNKDISRSFREEKDRSNKAEKERSLKEKSPKEEKLRLYKEERKKKSKDRPSKL 776
SP|E9Q4F7|ANR11_MOUSE VLKRIKDANKDMSRAFREDKDRASKAERERATKDKSPKEEKLRLYKEERKKKSKDRASRL 780
                        ******:***:**:***:***:.***:**: *:********************** *:*

SP|Q6UB99|ANR11_HUMAN EKKNDLKEDKISKEKEKIFKEDKEKLKKEKVYREDSAFDEYCNKNQFLENEDTKFSLSDD 836
SP|E9Q4F7|ANR11_MOUSE ERKNDMKEDKLSKEKEKAFKEDKEKLKKEKLYREDAAFDDYCNKSQFLDHEDTKFSLSDD 840
                       *:***:****:****** ************:****:***:****.***::**********

SP|Q6UB99|ANR11_HUMAN QRDRWFSDLSDSSFDFKGEDSWDSPVTDYRDMKSDSVAKLILETVKEDSKERRRDSRARE 896
SP|E9Q4F7|ANR11_MOUSE QQERWFSDLSDSSFDFKGEDSWDS-VTDYRDIKNDSVAKLILETVKEDSKEKKRDNKIRE 899
                       *::******************** ******:*.*****************::**.: **
```

```
SP|Q6UB99|ANR11_HUMAN KRDYREPFFRKKDRDYLDKNSEKRKEQTEKHKSVPGYLSEKDKKRRESAEAGRDRKDALE 956
SP|E9Q4F7|ANR11_MOUSE KRDFKDSFFRKRDRDCLDKNSEKRRDQTEKHKSIPSYLSEKDKKRRESAEGGRDR----- 954
                       ***::: ****:*** ********::*******:*.**************.****

SP|Q6UB99|ANR11_HUMAN SCKERRDGRAKPEEAHREELKECGCESGFKDKSDGDFGKGLEPWERHHPAREKEKKDGPD 1016
SP|E9Q4F7|ANR11_MOUSE -----RDGRIRSEEVHREDLKECGFESSFKDKSDCDFPKNLEPWERPHAAREKEKKDALE 1009
                            **** : **.***:***** **.****** ** *.****** * ********. :

SP|Q6UB99|ANR11_HUMAN KERKEKTKPERYKEKSSDKDKSEKSILEKCQKDKEFDKCFKEKKDTKEKHKDTHGKDKER 1076
SP|E9Q4F7|ANR11_MOUSE KERKEKGRADKYKEKSSERERSDKSTLDKCQKDKEFEKCFKEKKDGKEKHKDIHSKD--R 1067
                       ****** : ::******::::*:** *:********:******** ****** *.**  *

SP|Q6UB99|ANR11_HUMAN KASLDQGKEKKEKAFPGIISEDFSEKKDDKKGKEKSWYIADIFTDESEDDRDSCMGSGFK 1136
SP|E9Q4F7|ANR11_MOUSE KASFDQLREKKEKVFSSIISEDFSERKDDRKGKEKSWYIADIFTDESEDEKDDCVAGSFK 1127
                       ***:** :*****.* .********:***:*******************::*.*:...**

SP|Q6UB99|ANR11_HUMAN MGEASDLPRTDGLQEKEEGREAYASDRHRKSSDKQHPERQKDKEPRDRRKDRGAADAGRD 1196
SP|E9Q4F7|ANR11_MOUSE ATEASDTQRVDGLPEKEEGREHPSDRHRKSSSDRQHTEKPRDKEPKEKKKDRGASEGGKD 1187
                         ****  *.*** *******  :. :::.***:** *: :****::::*****::.*:*

SP|Q6UB99|ANR11_HUMAN KK---EKVFEKHKEKKDKESTEKYKDRKDRASVDSTQDKKNKQKLPEKAEKKHAAEDKAK 1253
SP|E9Q4F7|ANR11_MOUSE KKEKMEKIFEKHKEKKDKECAERYKDRKERASADSAPEKKNKQKLPEKVEKKHFAEDKVK 1247
                       **   **:***********.:*:*****:***.**: :**********.**** ****.*

SP|Q6UB99|ANR11_HUMAN SKHKEKSDKEHSKE--RKSSRSADAEKSLLEKLEEEALHEYREDSNDKISEVSSDSFTDR 1311
SP|E9Q4F7|ANR11_MOUSE SKHKEKPEKEHSRERERKPSRGPDVEKSLLEKLEEEALHDYREDSNDKISEVSSDSFADH 1307
                       ****** :****:*  ** **. *.**************:*****************:*:

SP|Q6UB99|ANR11_HUMAN GQEPGLTAFLEVSFTEPPGDDKPRESACLPEKLKEKERHRHSSSSSKKSHDRERAKKEKA 1371
SP|E9Q4F7|ANR11_MOUSE GQEPSLSTLLEVSFSEPPAEDKARDSACLSEKLREKERHRHSSSSSKKSHERERAKKEKA 1367
                       ****.*:::*****:***.:** *:**** ***:****************:*********

SP|Q6UB99|ANR11_HUMAN EKKEKGEDYKEG--GSRKDSGQYEKDFLEADAYGVSYNMKADIEDELDKTIELFSTEKKD 1429
SP|E9Q4F7|ANR11_MOUSE EKKEKSEDYKDSISSVRKDASQFEKDFLDAETYGVSYPTKADVEEELDKAIELFSSEKKD 1427
                       *****.****:.  . ***:.*:*****:*::*****  ***:*:****:*****:****

SP|Q6UB99|ANR11_HUMAN KNDSEREPSKKIEKELKPYGSSAINILKEKKKREKHREKWRDEKERHRDRHADGLLRHHR 1489
SP|E9Q4F7|ANR11_MOUSE RSDPEREPAKRIEKELKPYGSSAISILKEKKKREKHRERWREEKERHRDKHVDGFLRHH- 1486
                       :.* ****:*:*************.*************:**:*******:*.**:****

SP|Q6UB99|ANR11_HUMAN DELLRHHRDEQKPATRDKDSPPRVLKDKSRDEGPRLGDAKLKEKFKDGAEKEKGDPVKMS 1549
SP|E9Q4F7|ANR11_MOUSE -------KDEPKPAAKDKDNPPNSFKEKSREESLKLSETKLKEKFKENTEREKGDSIKMS 1539
                              :** ***::***.**. :*:***:*. :*.::*******:.:*:**** :***

SP|Q6UB99|ANR11_HUMAN NGNDKVAPSKDPGKKDARPREKLLGDGDLMMTSFERMLSQKDLEIEERHKRHKERMKQME 1609
SP|E9Q4F7|ANR11_MOUSE NGNDKLVPSRDSGKKDSRPREKLLGDGDLMMTSFERMLSQKDLEIEERHKRHKERMKQME 1599
                       *****:.**:* ****:****************************************

SP|Q6UB99|ANR11_HUMAN KLRHRSGDPKLKEKAKPADDGRKKGLDIPAKKPPGLDPPFKDKKLKESTPIPPAAENKLH 1669
SP|E9Q4F7|ANR11_MOUSE KMRHRSGDPKLKEK-KPTEDGRKKSLDFPSKKALGLDKK-----VKEPAPTLTTGESKPH 1653
                       *:************ **::*****.**:*:**  ***       :** :*   :.*.* *

SP|Q6UB99|ANR11_HUMAN PASGADSKDWLAGPHMKEVLPASPRPDQSRPTGVPTPTSVLSCPSYEEVMHTPRTPSCSA 1729
SP|E9Q4F7|ANR11_MOUSE SGPGTESKDWLSGQPLKEVLPASPRTEQSRPTGVPTPTSVVSCPSYEEVMHTPRTPSCSA 1713
                        . *::*****:*  :********* :*************:******************

SP|Q6UB99|ANR11_HUMAN DDYADLVFDCADSQHSTPVPTAPTSACSPSFFDRFSVASSGLSENA-SQAPARPLSTNLY 1788
SP|E9Q4F7|ANR11_MOUSE DDYPDLVFDCTDSQHSMPVSTASTSACSPPFFDRFSVASSVVSENAAGQTPTRPISTNLY 1773
                       *** ******:***** ** ** ****** ********** :**** .*:*:**:*****

SP|Q6UB99|ANR11_HUMAN RSVSVDIRRTPEEEFSVGDKLFRQQSVPAASSYDSPMPPSMEDRAPLPPVPAEKFACLSP 1848
SP|E9Q4F7|ANR11_MOUSE RSISVDIRRTPEEEFSAGDKLFRQQSVPAPSSFDSPVQHLLEEKAPLPPVPAEKFACLSP 1833
                       **:*************.************ **:***:   :*::****************

SP|Q6UB99|ANR11_HUMAN GYYSPDYGLPSPKVDALHCPPAAVVTVTPSPEGVFSSLQAKPSPSPRAELLVPSLEGALP 1908
SP|E9Q4F7|ANR11_MOUSE GYYSPDYGIPSPKVDTLHCPPTAVVSATPPPDSVFSNLPPKSSPSPRGELLSPAIEGTLP 1893
                       ********:******:*****:***:.** *:.***.*  * *****.*** *::**:**
```

```
SP|Q6UB99|ANR11_HUMAN PDLD----TSEDQQATAAIIPPEPSYLEPLDEGPFSAVITEEPVEWAHPSEQ--ALASSL 1962
SP|E9Q4F7|ANR11_MOUSE PDLGLPLDATEDQQATAAILPQEPSYLEPLDEGPFTTVITEEPVEWTHTAAEQGLSSSSL 1953
                      ***.    ::*********:* *************::*********:* : :    :***

SP|Q6UB99|ANR11_HUMAN IGGTSENPVSWPVGSDLLLKSPQRFPESPKRFCPADPLHSAAPGPFSASEAPYPAPPASP 2022
SP|E9Q4F7|ANR11_MOUSE IASASENPVSWPVGSELMLKSPQRFAESPKHFCPGESLHSTTPGPYSAAEPTYPV---SP 2010
                      *..:***********:*:******* ****:***.: ***::***:**:*  **.   **

SP|Q6UB99|ANR11_HUMAN APYALPVAEPGLEDVKDGV-DAVPAAIST-SEAAPYAPPSGLESFFSNCKSLPEAPLDVA 2080
SP|E9Q4F7|ANR11_MOUSE GSYPLPAPEPALEEVKDGGTGAIPVAISAAEGAAPYAAPARLESFFSNCKSHPDAPLDTA 2070
                      . * **. **.**:****  .*:*.***: . ***** *: ********** *:****.*

SP|Q6UB99|ANR11_HUMAN PEPACVAAVAQVEALGPLENSFLDGSRGLSHLGQVEPVPWADAFAGPEDDLDLGPFSLPE 2140
SP|E9Q4F7|ANR11_MOUSE PEPTGVTAVAQVEALGPLESSFLDSNPSISTLSQVEPVSWHEAFTSPEDDLDLGPFSLPE 2130
                      ***: *:************.****.. .:* *.***** * :**:.**************

SP|Q6UB99|ANR11_HUMAN LPLQTKDAADGEAEPVEESLAPPEEMPPGAPGVINGGDVSTVVAEEPPALPPDQASTRLP 2200
SP|E9Q4F7|ANR11_MOUSE LPLQAKDASDVEAEAAKASPVPPAESPPGPTGVLGGGDVPAPAAEEPPAPPPQEASPQLS 2190
                      ****:***:* *** .: * .** * ***  **:.**** : .****** **::** :*

SP|Q6UB99|ANR11_HUMAN AELEPEPSGEPKLDVALEAAVEAETVPEERARGDPDSSVEPAPVPPEQRPLGSGDQGAEA 2260
SP|E9Q4F7|ANR11_MOUSE --TEPEPSEEPKLDVVLEATVETEVLADDSAPEASISNSVPAPSPPQQQPPGGGDEEAET 2248
                         ***** ******.***:**:*.: :: *     *.  *** **:*:* *.**: **:

SP|Q6UB99|ANR11_HUMAN EGPPAASLCAPDGPAPNTVAQAQAADGAGPEDDTEASRAAAPAEGPPGGIQPEAA--EPK 2318
SP|E9Q4F7|ANR11_MOUSE EDPSATPCCAPDGPTTDGLAQAHN--------SAEASCVVAAAEGPPGNVQAEATDPEPK 2300
                      *.* *:  ******: : :***:         .:*** ..* ******.:* **:  ***

SP|Q6UB99|ANR11_HUMAN PTAEAPKAPRVEEIPQRMTRNRAQMLANQSKQGPPPSEKECAPTPAPVTRAKARGSEDDD 2378
SP|E9Q4F7|ANR11_MOUSE PTSEVPKAPKVEEVPQRMTRNRAQMLASQSKQGIPAAEKDP--MPTPASRAKGRASEEED 2358
                      **:*.****:***:*************.***** * :**:    *:*.:***.*.**::*

SP|Q6UB99|ANR11_HUMAN AQAQHPRKRRFQRSTQQLQQQLNTSTQQTREVIQQTLAAIVDAIKLDAIEPYHSDRANPY 2438
SP|E9Q4F7|ANR11_MOUSE AQAQHPRKRRFQRSSQQLQQQLNTSTQQTREVIQQTLAAIVDAIKLDAIEPYHSDRSNPY 2418
                      **************:*******************************************:***

SP|Q6UB99|ANR11_HUMAN FEYLQIRKKIEEKRKILCCITPQAPQCYAEYVTYTGSYLLDGKPLSKLHIPVIAPPPSLA 2498
SP|E9Q4F7|ANR11_MOUSE FEYLQIRKKIEEKRKILCCITPQAPQCYAEYVTYTGSYLLDGKPLSKLHIPVIAPPPSLA 2478
                      ************************************************************

SP|Q6UB99|ANR11_HUMAN EPLKELFRQQEAVRGKLRLQHSIEREKLIVSCEQEILRVHCRAARTIANQAVPFSACTML 2558
SP|E9Q4F7|ANR11_MOUSE EPLKELFKQQEAVRGKLRLQHSIEREKLIVSCEQEILRVHCRAARTIANQAVPFSACTML 2538
                      *******:****************************************************

SP|Q6UB99|ANR11_HUMAN LDSEVYNMPLESQGDENKSVRDRFNARQFISWLQDVDDKYDRMKTCLLMRQQHEAAALNA 2618
SP|E9Q4F7|ANR11_MOUSE LDSEVYNMPLESQGDENKSVRDRFNARQFISWLQDVDDKYDRMKTCLLMRQQHEAAALNA 2598
                      ************************************************************

SP|Q6UB99|ANR11_HUMAN VQRMEWQLKVQELDPAGHKSLCVNEVPSFYVPMVDVNDDFVLLPA 2663
SP|E9Q4F7|ANR11_MOUSE VQRMEWQLKAQELDPAGHKSLCVNEVPSFYVPMVDVNDDFVLLPA 2643
                      *********.**********************************
```

Figure S3: Four variants are located at three residues in predicted destruction motifs

ANKRD11 amino acid sequence with the variants identified in affected individuals shaded in yellow. Different degradation motifs are indicated: RxxL-motifs are underlined, Proviz-predicted destruction motifs are bold, with D-boxes in red, Ken-boxes in green and an Abba-motif in orange.

>sp|Q6UB99|ANR11_HUMAN Ankyrin repeat domain-containing protein 11 OS=Homo sapiens OX=9606 GN=ANKRD11 PE=1 SV=3

MPKGGCPKAPQQEELPLSSDMVEKQTGKKDKDKVSLTKTPKLERGDGGKEVRERASKRKL
PFTAGANGEQKDSDTEKQGPERKRIKKEPVTRKAGLLFGMGLSGIRAGYPLSERQQVALL
MQMTAEESANSPVDTTPKHPSQSTVCQKGTPNSASKTKDKVNKRNERGETRLHRAAIRGD
ARRIKELISEGADVNVKDFAGWTALHEACNRGYYDVAKQLLAAGAEVNTKGLDDDTPLHD
AANNGHYKVVKLLLRYGGNPQQSNRKGETPLKVANSPTMVNLLLGKGTYTSSEESSTESS
EEEDAPSFAPSSSVDGNNTDSEFEKGLKHKAKNPEPQKATAPVKDEYEFDEDDEQDRVPP
VDDKHLLKKDYRKETKSNSFISIPKMEVKSYTKNNTIAPKKASHRILSDTSDEEDASVTV
GTGEKLRLSAHTILPGSKTREPSNAKQQKEKNKVKKKRKKETKGREVRFGKRSDKFCSSE
SESESSESGEDD**RDSL**GSSGCLKGSPLVLKDPSLFSSLSASSTSSHGSSAAQKQNPSHTD
QHTKHWRTDNWKTISSPAWSEVSSLSD**STRTRLTSESDY**SSEGSSVESLKPVRKRQEH**RK**
RASLSEKKSPFLSSAEGAVPKLDKEGKVVKKHKTKHKHKNKEKGQCSISQELKLKSFTYE
YEDSKQKSDKAILLENDLSTENKLKVLKHDRDHFKKEEKLSKMKLEEKEWLFKDEKSLKR
IKDTNKDISRSFREEKDRSNKAEKERSLKEKSPKEEKLRLYKEERKKKSKDRPSKL**EKKN**
DLKEDKISKEKEKIFKEDKEKLKKEKVYREDSAFDEYCNKNQFLENEDT**KFSLSDD**QRDR
WFSDLSDSSFDFKGEDSWDSPVTDYRDMKSDSVAKLILETVKEDSKERRRDSRAREKRDY
REPFFRKKD**RDYL**DKNSEKRKEQTEKHKSVPGYLSEKDKKRRESAEAGRDRKDALESCKE
RRDGRAKPEEAH**REEL**KECGCESGFKDKSDGDFGKGLEPWERHHPAREKEKKDGPDKERK
EKTKPERYKEKSSDKDKSEKSILEKCQKDKEFDKCFKEKKDTKEKHKDTHGKDKERKASL
DQGKEKKEKAFPGIISEDFSEKKDDKKGKEKSWYIADIFTDESEDDRDSCMGSGFKMGEA
SDLPRTDGLQEKEEGREAYASDRHRKSSDKQHPERQKDKEPRDRRKDRGAADAGRDKKEK
VFEKHKEKKDKESTEKYKDRKDRASVDSTQ**DKKNKQK**LPEKAEKKHAAEDKAKSKHKEKS
DKEHSKERKSSRSADAEKSLLEKLEEEALHEYREDSNDKISEVSSDSFTDRGQEPGLTAF
LEVSFTEPPGDDKPRESACLPEKLKEKERHRHSSSSSKKSHDRERAKKEKAEKKEKGEDY
KEGGSRKDSGQYEKDFLEADAYGVSYNMKADIEDELDKTIELFSTEKKDKNDSEREPSKK
IEKELKPYGSSAINILKEKKKREKHREKWRDEKERHRDRHADGLLRHH**RDEL**LRHHRDEQ
KPATRDKDSPPRVLKDKSRDEGPRLGDAKLKEKFKDGAEKEKGDPVKMSNGNDKVAPSKD
PGKKDARP**REKL**LGDGDLMMTSFERMLSQKDLEIEERHKRHKERMKQMEKLRHRSGDPKL
KEKAKPADDGRKKGLDIPAKKPPGLDPPFKDKKLKESTPIPPAAENKLHPASGADSKDWL
AGPHMKEVLPASPRPDQSRPTGVPTPTSVLSCPSYEEVMHTPRTPSCSADDYADLVFDCA
DSQHSTPVPTAPTSACSPSFFDRFSVASSGLSENASQAPARPLSTNLYRSVSVDIRRTPE
EEFSVGDKLFRQQSVPAASSYDSPMPPSM**EDRAPLPPVPAE**KFACLSPGYYSPDYGLPSP
KVDALHCPPAAVVTVTPSPEGVFSSLQAKPSP**SPRAELLVPSLE**GALPPDLDTSEDQQAT
AAIIPPEPSYLEPLDEGPFSAVITEEPVEWAHPSEQALASSLIGGTSENPVSWPVGSDLL
LKSPQRFPESPKRFCPADPLHSAAPGPFSASEAPYPAPPASPAPYALPVAEPGLEDVKDG
VDAVPAAISTSEAAPYAPPSGLESFFSNCKSLPEAPLDVAPEPACVAAVAQVEALGPLEN
SFLDGSRGLSHLGQVEPVPWADAFAGPEDDLDLGPFSLPELPLQTKDAADGEAEPVEESL
APPEEMPPGAPGVINGGDVSTVVAEEPPALPPDQASTRLPAELEPEPSGEPKLDVALEAA
VEAETVPEERARGDPDSSVEPAPVPPEQRPLGSGDQGAEAEGPPAASLCAPDGPAPNTVA
QAQAADGAGPEDDTEASRAAAPAEGPPGGIQPEAAEPKPTAEAPKAPRVEEIPQRMTRNR
AQMLANQSKQGPPPSEKECAPTPAPVTRAKARGSEDDDAQAQHPRKRRFQRSTQQLQQQL
NTSTQQTREVIQQTLAAIVDAIKLDAIEPYHSDRANPYFEYLQIRKKIE**EKRKILCCITP**
QAPQCYAEYVTYTGSYLLDGKPLSKLHIPVIAPPPSLAEPLKELFRQQEAV**RGKL**RLQHS
IEREKLIVSCEQEILRVHCRAARTIANQAVPFSACTMLLDSEVYNMPLESQ**GDENKSVR**D
RFNARQFISWLQDVDDKYDRMKTCLLMRQQHEAAALNAVQRMEWQLKVQELDPAGHKSLC
VNEVPSFYVPMVDVNDDFVLLPA

Figure S4: *ANKRD11* missense variants affecting arginine residues in RD2 are overrepresented in the cohort

The observed number of mutated arginine residues in our cohort (12/17 RD2; 0/8 outside RD2) were compared against an expected distribution of mutated arginine residues in ANKRD11 (see Methods). The mean (circle) and standard deviation (interval) of the expected distribution is shown in red. The black diamond represents the observed distribution inside RD2 (top) and outside (bottom). Permutation *p*-values shown above the expected distribution represent the likelihood that the observed distribution would occur by chance.

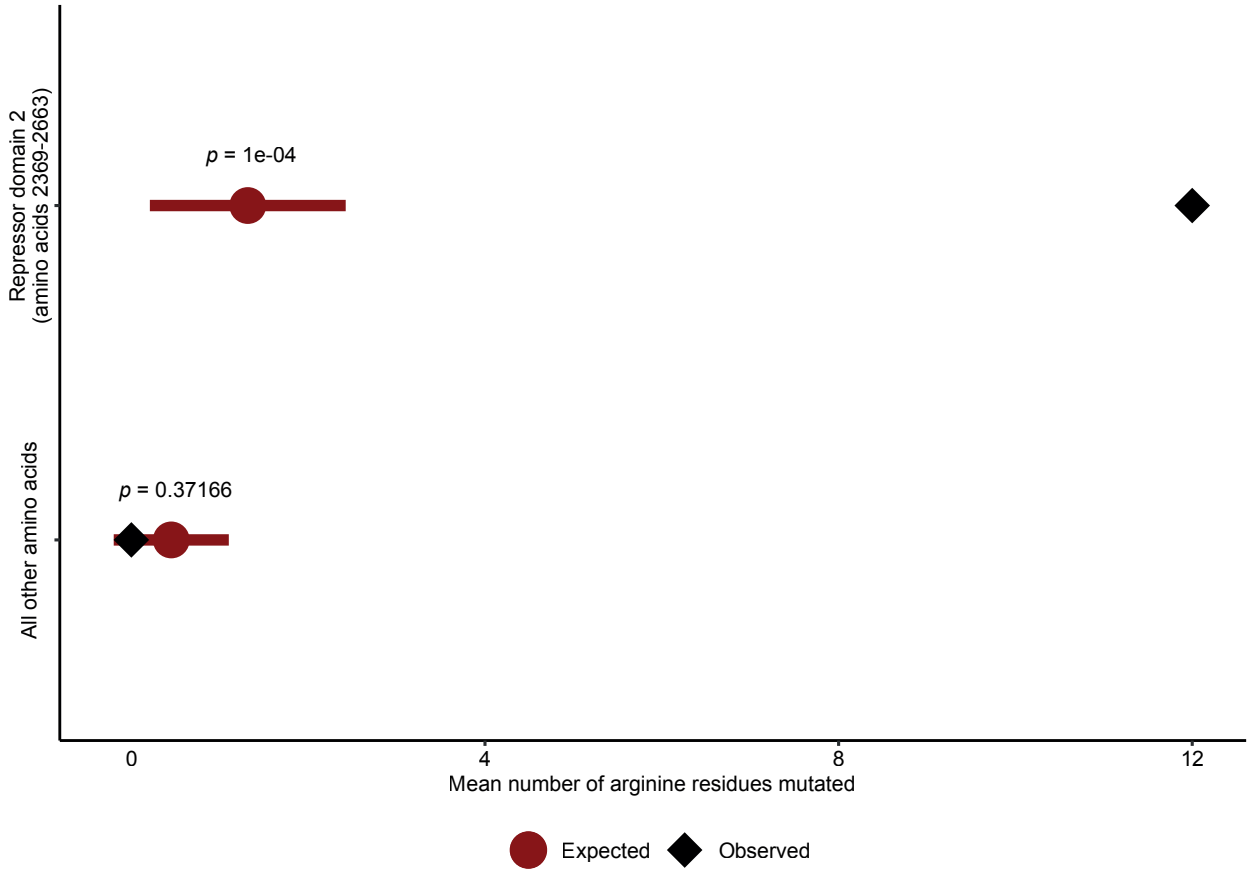

Figure S5: Quantification of ANKRD11 nuclear speckles (related to Figure 3)

Results of quantification of (A) number, (B) size, (C) perimeter, (D) area covered, (E) solidity and (F) and density of ANKRD11 nuclear speckles. Values are expressed relative to wildtype (WT) and represent the mean ± SD of three independent experiments (one-way ANOVA and a post-hoc Dunnett's test).

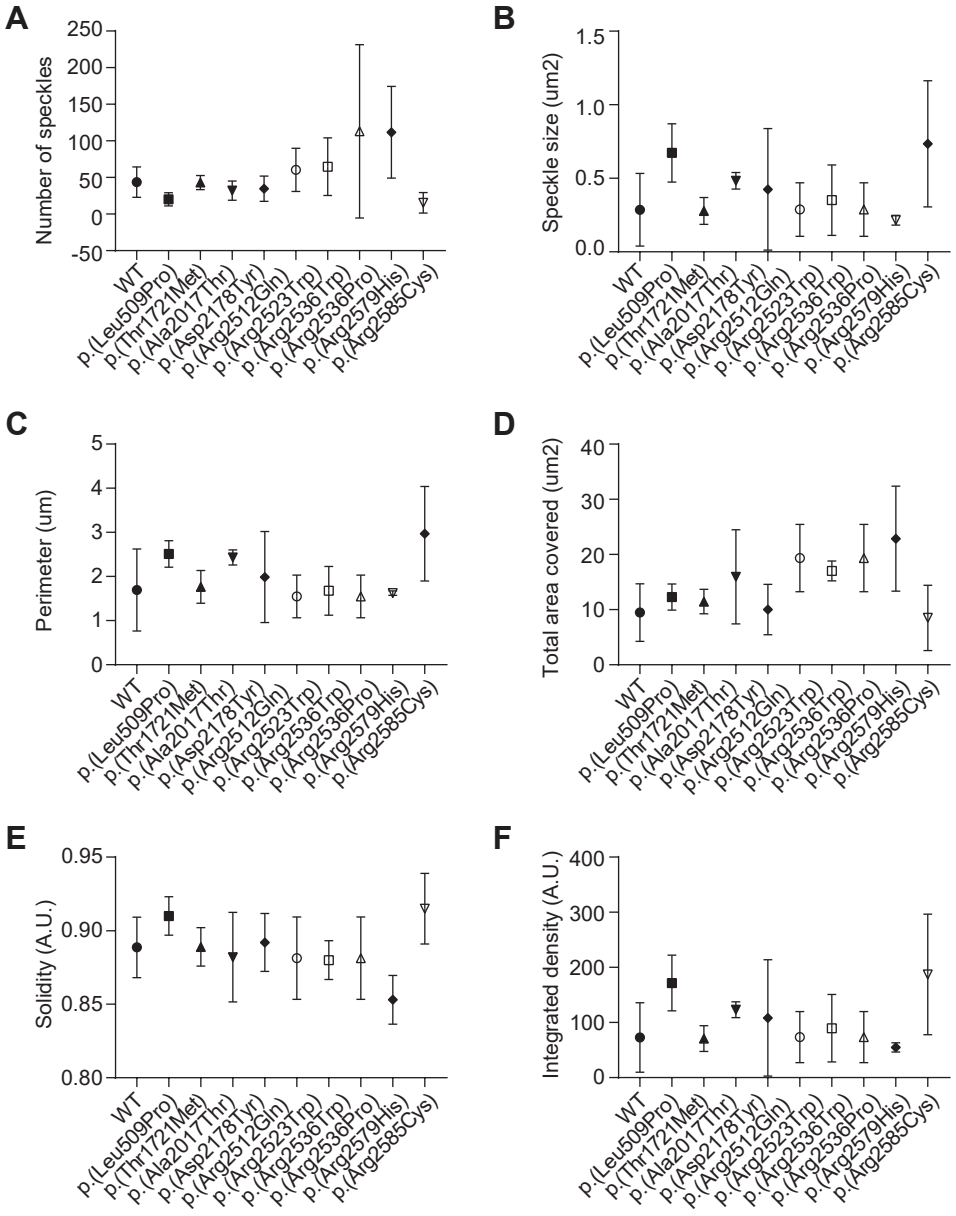

Figure S6: EGFP-ANKRD11 protein expression in transiently transfected HEK293T/17 cells

(A) Immunoblot of whole cell lysates of HEK293T/17 cells expressing EGFP-Myc-tagged ANKRD11 variants probed with an anti-GFP antibody. B) Immunoblot of whole cell lysates of HEK293T/17 cells expressing EGFP-Myc-tagged ANKRD11 variants probed with an anti-Myc antibody. β-actin was used as a loading control.

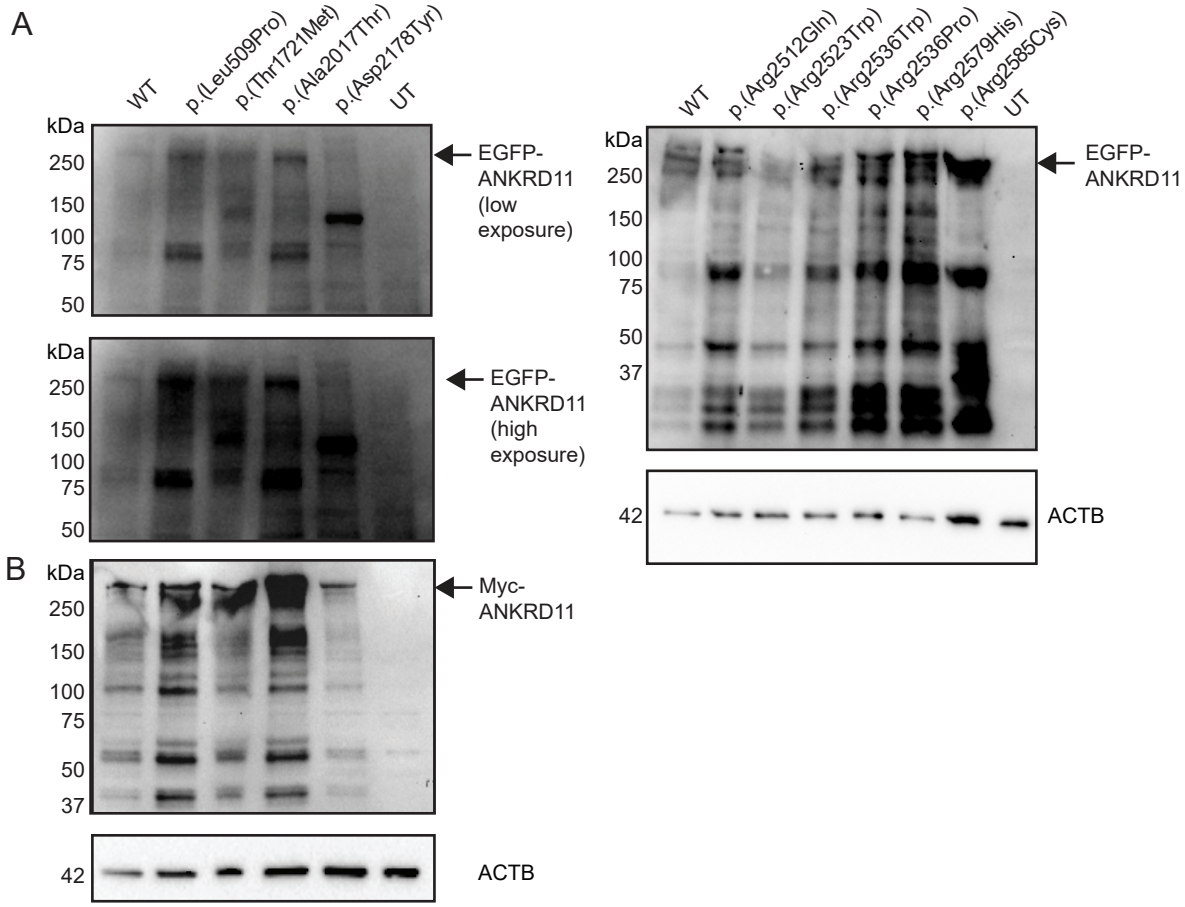

Figure S7: Stability and degradation of ANKRD11 variants as EGFP-fusion protein in HEK293T/17 cells

Relative expression ANKRD11 variants as EGFP-fusion protein in HEK293T/17 cells treated with (A) 50µg/ml cycloheximide (CHX) or (B) 5µg/ml proteasome inhibitor MG132. Equal volume of DMSO was used as a vehicle control. Fluorescence intensity was measured for 24 hours with three-hour intervals. Values are expressed relative to t= 0 hour and represent the mean ± SD of three independent experiments, each preformed in triplicates (*p<0.05, **p<0.01, ***p<0.001, ****p<0.0001 CHX or MG132 versus DMSO; repeated measure two-way ANOVA and a post-hoc Sidak's test).

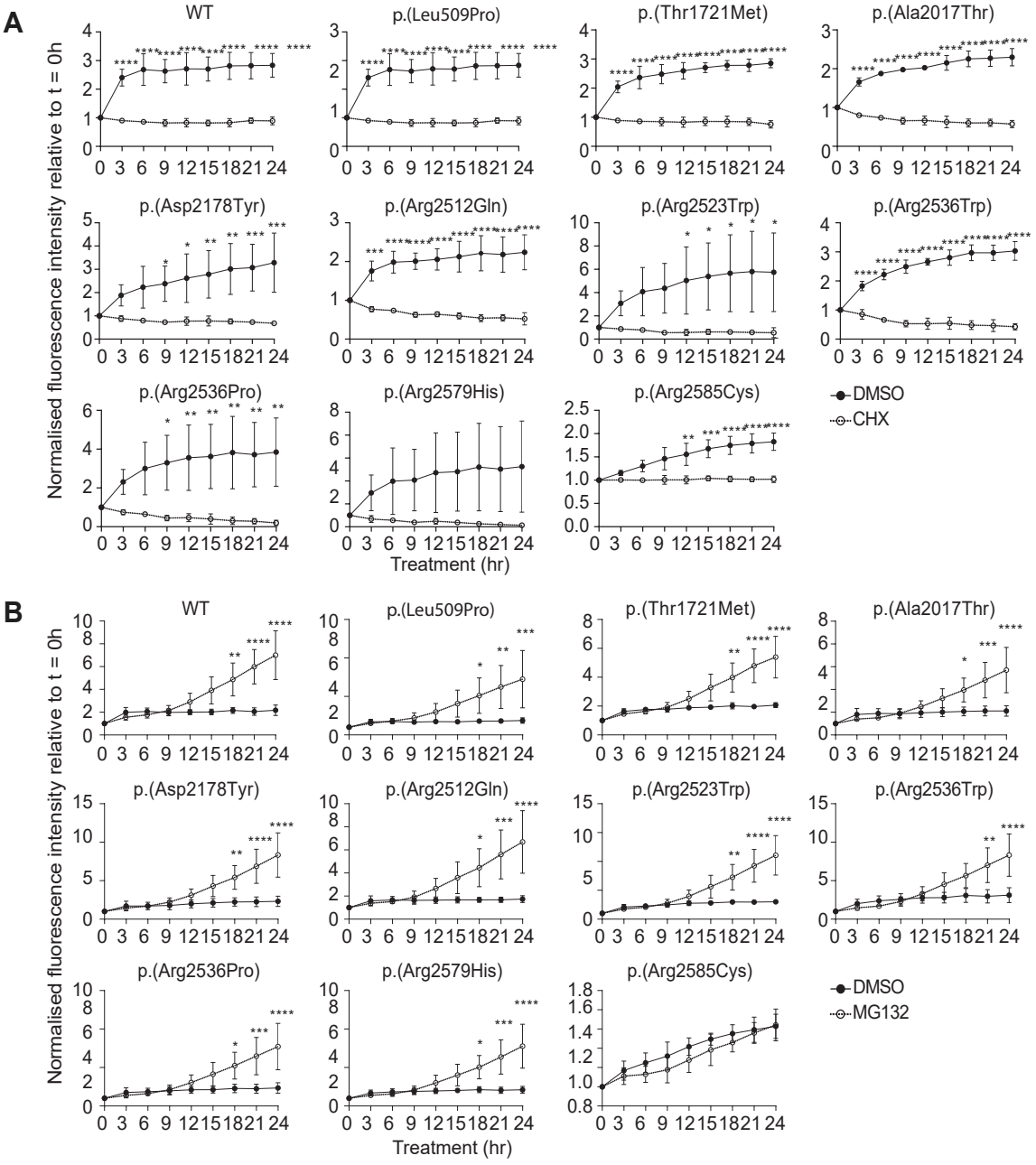

Figure S8: Potential effects on cryptic splice sites

Alamut splice site tools predict potential effects of p.(Gly1093Arg) and p.(Asp2178Tyr), respectively predicted to remove a cryptic acceptor splice site, and to introduce a cryptic donor splice site.